International Conferences on Recent Advances in Geotechnical Earthquake Engineering and Soil Dynamics

1981 - First International Conference on Recent Advances in Geotechnical Earthquake Engineering & Soil Dynamics

28 Apr 1981, 9:00 am - 12:30 pm

Liquefaction Analysis of Sand Deposits Based on Cyclic Elasto-Piasticity

F. Oka
Gifu University, Japan

T. Murase
Nippon Doro Co. Ltd., Japan

Proceedings: First International Conference on Recent Advances in Geotechnical Earthquake Engineering and Soil Dynamics, April 26 - May 3, 1981, St. Louis, Missouri

Liquefaction Analysis of Sand Deposits Based on Cyclic Elasto-Plasticity

F. Oka
Associate Professor, Department of Civil Engineering, Gifu University, Kakamigahara, Gifu, Japan

T. Murase
Engineer, Nippon Doro Co. Ltd., Otaru, Japan

SYNOPSIS The one-dimentional liquefaction analysis of sand deposits is performed by using the theory of two-phase mixture and the elasto-plastic constitutive equations of sand that can describe the dynamic dilatancy effect of soil under cyclic loading. The analytical results obtained by finite difference method explain well the dynamic behavior of sand deposits including liquefaction phenomena. Especially, the stress path which is particular to liquefaction is presented by considering a horizontally confined condition.

INTRODUCTION

Recently, many analytical studies of liquefaction have been performed by various different methods. Despite remarkable achievements in the liquefaction analysis, there are several major problems to be solved, in relation to the constitutive relations of soil and in-situ conditions of actual soil deposits. In order to predict the liquefaction phenomena with a high accuracy, the realistic constitutive relations of soil, which are capable of describing the mechanical behavior under repeated stress reversals, are needed. In this present study, the constitutive equation of sand, newly developed by one of the authors(Oka, F. et al.,1981), is applied to liquefaction analysis, which is described in another paper to this conference.

On the other hand, it should be pointed out that the horizontal deformation is confined in the actual grounds. Then, the ratio of the horizontal stress to the vertical stress will vary during the shaking caused by earthquakes. In the present paper, the horizontal deformation confined condition is taken into account.

It is well known that the pore water pressure generated during the cyclic loading dissipates into the ground through seepage. Here, the dissipation of pore water pressure is estimated by introducing the Darcy's type interaction between the pore water and soil skelton. The theory of two-phase mixture proposed by oka (1978) and the stress-strain relation of sand are used to numerically analyze the dynamic behavior of saturated sand deposits by finite difference method.

CONSTITUTIVE EQUATION OF SAND

The constitutive equation of sand is derived based on the elasto-plastic theory and the concept of a bounding surface which denotes the boundary between normally consolidated region and overconsolidated region. The detailed description of the constitutive equation is reported in another paper in this conference (Oka et al. 1981).
The boundary surface is given by the following equation.

$$f_b = \bar{\eta}^*_{(0)} + M^*_m \ln(\sigma'_m/\sigma'_{me}) = 0 \qquad (1)$$

where σ'_m is a mean effective stress, σ'_{me} is a preconsolidation pressure and $\bar{\eta}^*$ is a stress parameter proposed by Sekiguchi & Ohta(1977), and is given by

$$\bar{\eta}^*_{(0)} = [(\eta^*_{ij} - \eta^*_{ij(0)})(\eta^*_{ij} - \eta^*_{ij(0)})]^{1/2} \qquad (2)$$

$$\eta^*_{ij} = s_{ij}/\sigma'_m \qquad (3)$$

In Eqs.(2) and (3), s_{ij} is a deviatoric stress tensor and $\eta^*_{ij(0)}$ denotes the value of η^*_{ij} at the end of anisotropic consolidation. In Eq.(1), M^*_m is a value of $(\eta^*_{ij}\eta^*_{ij})^{1/2}$ when the maximum compression takes place.
The plastic strain rate tensor $d\varepsilon^p_{ij}$ is given by the non-associated flow rule,

$$d\varepsilon^p_{ij} = \Lambda \frac{\partial f_p}{\partial \sigma_{ij}} df \qquad (4)$$

where σ_{ij} is a stress tensor, f_p is a plastic potential and f is a yield function as follows.

$$f = \bar{\eta}^* \qquad (5)$$

The plastic potential is given by

$$f_p = \bar{\eta}^* + \tilde{M}^* \ln(\sigma'_m/\sigma'_{m(n)}) \qquad (6)$$

$$M^* = -\eta^*/\ln(\sigma'_m/\sigma'_{mc}) \quad (7) \qquad \eta^* = (\eta^*_{ij}\eta^*_{ij})^{1/2} \quad (8)$$

where $\bar{\eta}^* = [(\eta^*_{ij} - \eta^*_{ij(n)})(\eta^*_{ij} - \eta^*_{ij(n)})]^{1/2}$,

$\eta^*_{ij(n)}$ and $\sigma'_{m(n)}$ denote the values of η^*_{ij} and σ'_m at the n-th times turning over point of loading direction. σ'_{mc} is a value of $\sigma'_m \exp(\eta^*/M^*_m)$ at the end of consolidation.
We assume that the hardening rule is given by the following equations.

$$\bar{\gamma}^* = \frac{\bar{\eta}^*(M^*_f + \eta^*_{(n)})}{G'(M^*_f + \eta^*_{(n)} - \bar{\eta}^*)} \qquad (9)$$

$$\bar{\gamma}^* = [(e^p_{ij} - e^p_{ij(n)})(e^p_{ij} - e^p_{ij(n)})]^{1/2} \qquad (10)$$

where e^p_{ij} is the plastic deviatoric strain tensor, γ^* is a rlative strain and M^*_f is a value of η^* at failure, $\eta^*_{(n)}$ and $e^p_{ij(n)}$ denote the values of e^p_{ij} and $\eta^{*(n)}$ when n-times reverse loading takes place.
Finally, Λ is determined by Eqs.(4),(5),(6) and (9). The constitutive equations include eight soil parameters.
The following failure conditions are introduced.

$$\eta^* = M^*_f \quad (11), \quad |\varepsilon^p_{12}| \geq 0.05 \quad (12), \quad \sigma'_m \leq 0.05\,\sigma'_{m(0)} \quad (13)$$

where $\sigma'_{m(0)}$ is an initial value of σ'_m.
Eqs.(12) and (13) are used because of the restriction of numerical calculations.
The elastic strain rate tensor $d\varepsilon^e_{ij}$ is given by

$$d\varepsilon^e_{ij} = \frac{1}{2G} ds_{ij} + \frac{\kappa}{(1+e)\sigma'_m} d\sigma'_m \frac{1}{3}\delta_{ij} \quad (14)$$

where G is a elastic shear modulus, e is a void ratio and κ is a swelling index.

After failure, the constitutive equation of soil is replaced by the bilinear stress-strain relations.

$$\sigma'_{12} = 2G\varepsilon_{12} \,(|\sigma'_{12}| \leq \sigma'_{12y}), \quad \sigma'_{12} = 2\bar{G}\varepsilon_{12} \,(|\sigma'_{12}| > \sigma'_{12y}) \quad (15)$$

where σ'_{ij} is a effective stress tensor.

LIQUEFACTION ANALYSIS OF SAND DEPOSITS

Dynamic response of horizontally layered sand deposits is one-dimensionally analyzed in conjunction with the liquefaction. The ground is composed of elastic soil layers and the saturated elastic-plastic layers. Fig.1 denotes the ground model.

The one-dimensional approximated equation of motion for solid phase and kinematic equation, which were originally derived by one of the authors(Goto, et al.,1978, Oka, et al.,1980), are written by

$$\frac{\partial \sigma'_{12}}{\partial x_1} = \rho \frac{\partial v_2}{\partial t} \quad (16)$$

$$\frac{1}{2} \frac{\partial U_2}{\partial x_1} = -\varepsilon_{12} \quad (17)$$

where v_i is a component of velocity vector, U_i is a component of displacement vector, ε_{ij} is a strain tensor and ρ is a bulk density of soil.

If we can neglect the acceleration term, the following equation is obtained from the equation of mass conservation and equation of motion for fluid phase.

$$\frac{\partial^2 u}{\partial x_1^2} = -\frac{\rho^f g}{k} \frac{d\varepsilon_{kk}}{dt} \quad (18)$$

where u is a excess pore water pressure, ρ^f is a specific density of water, g is a gravitational acceleration, k is a permeability coefficient.

Generally, the horizontal deformation is quite small in the actual level ground during earthquake. Then, it is assumed that the horizontal deformation is zero.

$$d\varepsilon_{22} = d\varepsilon_{33} = 0 \quad (19)$$

From Eqs.(4),(14) and (19),we have

$$\frac{d\sigma'_{11}}{dt} = -K\left(\frac{k}{\rho^f g}\frac{\partial^2 u}{\partial x_1^2} + \frac{d\varepsilon^s_{kk}}{dt}\right) - 4G\left(\frac{1}{3}\frac{k}{\rho^f g}\frac{\partial^2 u}{\partial x_1^2} - \frac{de^p_{33}}{dt}\right) \quad (20)$$

$$\frac{d\sigma'_{33}}{dt} = -K\left(\frac{k}{\rho^f g}\frac{\partial^2 u}{\partial x_1^2} + \frac{d\varepsilon^s_{kk}}{dt}\right) + 2G\left(\frac{1}{3}\frac{k}{\rho^f g}\frac{\partial^2 u}{\partial x_1^2} - \frac{de^p_{33}}{dt}\right) \quad (21)$$

where $d\varepsilon^s_{kk}$ is a volumetric strain increment due to dilatancy, and $K = \frac{(1+e)\sigma'_m}{\kappa}$.

The above mentioned condition may be called "horizontally confined condition".

In order to obtain the solutions, we must solve the Eqs.(4),(13)-(21) simultaneously. The finite difference method is used for numerical calculations combined with the method of characteristics.

NUMERICAL EXAMPLES

The depth of the ground model is 30 m and the water table is at the depth of 2 m. The base rock is impermeable and drainage is allowed only in the upward direction. The soil properties for computation is similar to Niigata site where serious damage occrred, which is used by Seed & Idriss(1967). Distributions of shear modulus G and relative density D_r are shown in Fig.2 The base rock under the depth of 30 m is treated as a linear elastic body. The effect of scattering through base rock is also taken into account. The permeability k is determined by the formula $k = Ce^3/(1+e)$ (C; constant ,e;void ratio). G is proportional to $\sqrt{\sigma'_m}$.
The other parameters are as follows.

$\sqrt{\frac{3}{2}}M^*_m = 0.640$, $\sqrt{\frac{3}{2}}M^*_f = 0.739$, $\kappa = 0.003$, $e_{min} = 0.634$

$e_{max} = 0.991$, $\Delta x_1 = 1$ m, $\Delta t = 0.0025$sec, $\bar{G} = 5$ kgf/cm^2

$\sigma'_{12y} = 0.05$kgf/cm^2, $c_{(base\ rock)} = (\sqrt{\frac{G}{\rho}}) = 600$ m/sec

$\rho_{(base\ rock)} = 234$ kg sec^2/m^4 , $\lambda = 0.0098$

Case A $k = 10^{-2}$cm/sec, Case B $k = 2\times 10^{-2}$cm/sec

In case A, the incident wave at the depth of 30 m is calculated by Eq.(22)

$$V_2 = V_0 \sin(2\pi f_1 t)\sin(2\pi f_2 t) \quad (22)$$

$f_1 = 0.05$, $f_2 = 1.8$

Case A-1, $V_0 = 0.006$ m/sec

Case A-2, $V_0 = 0.06$ m /sec

On the other hand, in case B, a recorded accelerogram has been integrated to generate velocity and has been used as a incident wave at the depth od 30 m. The initial 10 sec of S69E component of accelerogram at Taft(1952) is used. In case B, the amplitude of velocity used for computation is 0.15 times as that of original record.

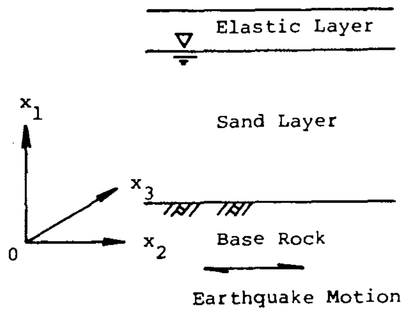

Fig.1 Model of Soil Layer

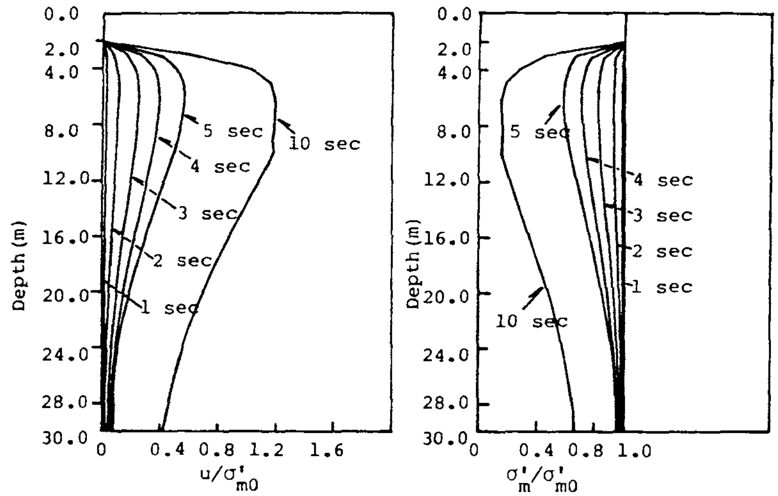

Fig.3 Distribution of excess pore water pressure and effective mean stress (case A)

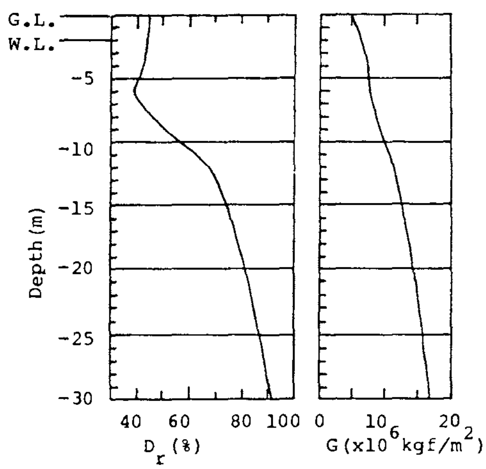

Fig.2 Distribution of D_r and G

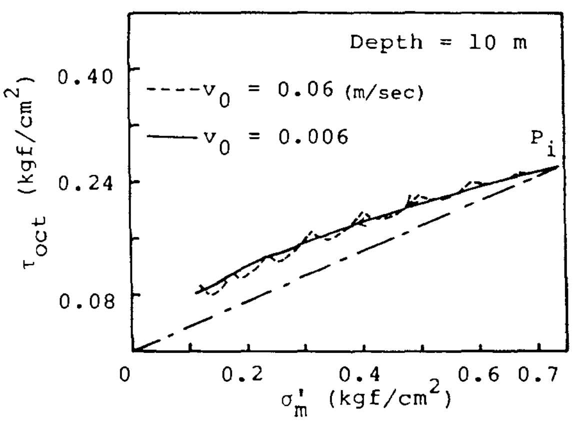

Fig.4 Stress Path (case A)

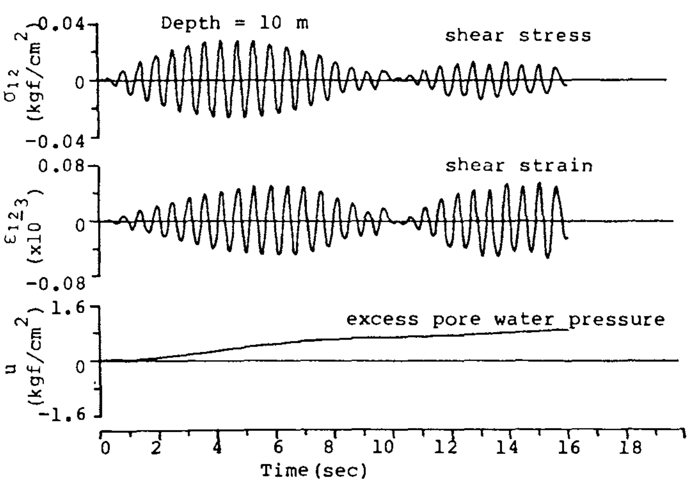

Fig.5 Time Histories of Liquefaction (case A-1)

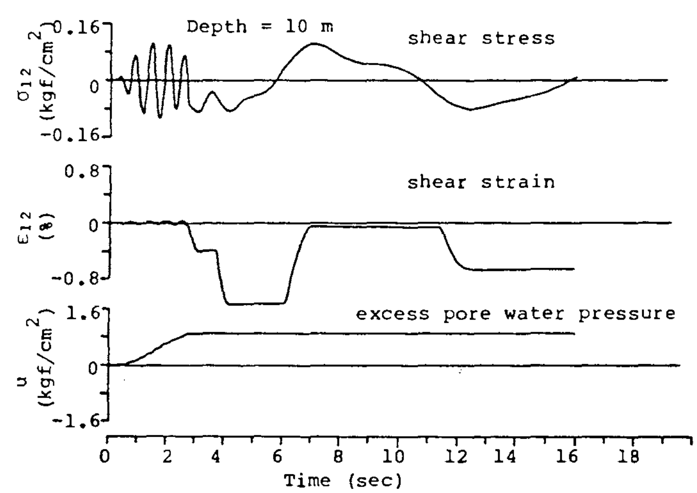

Fig.6 Time Histories of Liquefaction (case A-2)

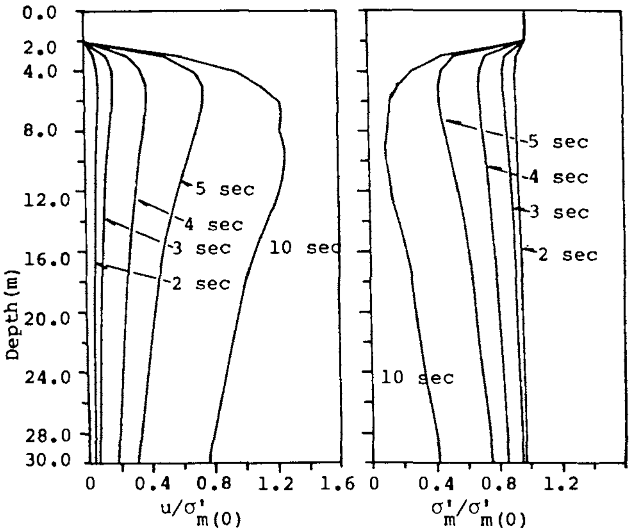

Fig.7 Distribution of excess pore water pressure and effective mean stress (case B)

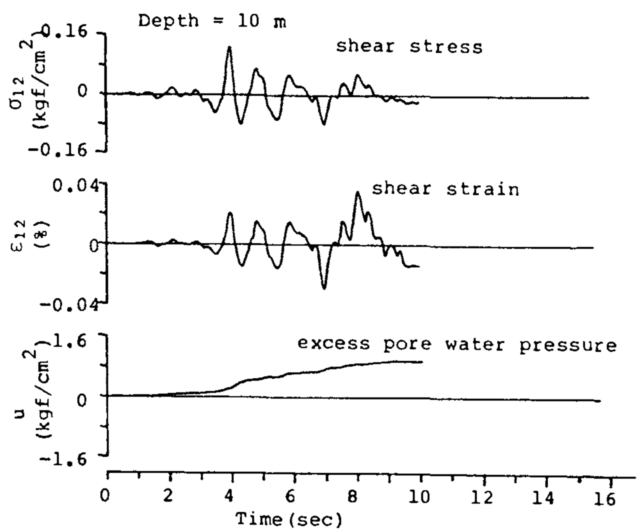

Fig.8 Time Histories of Liquefaction (case B)

Fig.3 shows the vertical distributions of excess pore water pressure and mean effective stress for case A-1. The maximum excess water pressure is obtained at a depth of 8 m in the calculation. The stress paths at a depth of 10 m in case of A-1 and in case of A-2 are shown in Fig.4. The point P_i represents the initial stress condition. This figure demonstrates the pattern of stress path that is particular to the liquefaction process, i.e., σ'_m decreases with the decrease in τ_{oct} (octahedral shear stress) and the stress path turns toward the origin. This characteristics of the stress path is mainly due to the horizontally confined condition by Eq.(19). In Figs.5 and 6, the shear stress, shear strain and excess pore water pressure at a depth of 10 m in cases of A-1 and A-2 are shown respectively. In Fig.6, the shear strain increases rapidly as the failure occurs and the excess pore water pressure gradually increases with time. In case A-1, the failure does not occur because that maginitude of input velocity wave is smaller than that in case of A-2.

Fig.7 shows the distributions of excess pore water pressure and mean effective stress in case B. The shear stress, shear strain and pore water pressure at a depth of 10 m in case B are shown in Fig.8. These trends are similar to those of case A in Figs.7 and 8.

CONCLUSIONS

A method of liquefaction analysis of saturated sand deposits has been developed by using the constitutive equation of sand that can express the dilatancy effect during cyclic loads and the theory of two-phase mixture. Especially, the stress path that is particular to the liquefaction, is obtained by considering a horizontally confined condition. On the other hand, in the future work, the detailed study of the hardening rule which is applicable for more general stress path which includes stress reversal is required, in order to predict the liquefaction phenomena with a high accuracy.

ACKNOWLEDGEMENTS

The authors wish to thank Prof. H.Goto and Prof. H.Kameda of Kyoto Univ. and Prof. T.Adachi of Disaster Prevention Research Institute of Kyoto Univ. for their support and helpful discussions.

REFERENCES

Goto, H,F. Oka and K. Kawamoto(1978),"Liquefaction of soil and dynamic response of ground", Proc. of 5th Japan Earthquake Engng. Symp., Dec., pp.673-680.

Oka, F.(1978),"Constitutive theory for solid-fluid mixture and its application to stress wave propagation through cohesive soil", Proc. of JSCE, Vol.272, Apr., pp.117-130.

Oka, F. and S. Sekiguchi(1980),"Liquefaction analysis of horizontally layered sand considering a laterally confined condition", Proc. of 7th World conference on Earthquake Engineering, Istanbul, Vol.3, pp.125-128.

Oka, F. and H. Washizu(1981),"Constitutive equation for sands and overconsolidated clays under dynamic loads based on elasto-plasticity", Int. Conference on Recent Advances in Geotechnical Earthquake Engineering and Soil Dynamics", St.Louis, Missouri, USA, in printing.

Seed, H.B. and I.M. Idriss(1967),"Analysis of soil liquefaction: Niigata Earthquake", Proc. of ASCE, Vol.93, No.SM3, pp.83-108.

Sekiguchi, H. and H. Ohta(1977),"Induced anisotropy and time dependency in clays", Proc. Specialty Session 9, 9th ICSMFE, Tokyo, pp.229-238.